NRIAG Journal of Astronomy and Geophysics 7 (2018) 155–161

Contents lists available at ScienceDirect

NRIAG Journal of Astronomy and Geophysics

journal homepage: www.elsevier.com/locate/nrjag

Full length article

Texture analysis of aeromagnetic data for enhancing geologic features using co-occurrence matrices in Elallaqi area, South Eastern Desert of Egypt

Ahmed M. Eldosouky [a,*], Sayed O. Elkhateeb [b]

[a] Egyptian Environmental Affairs Agency (E.E.A.A.), Egypt
[b] Department of Geology, Faculty of Science, South Valley University, 83523 Qena, Egypt

ARTICLE INFO

Article history:
Received 1 July 2017
Revised 21 December 2017
Accepted 24 December 2017
Available online 28 December 2017

Keywords:
Aeromagnetic data
CO-occurrence matrices
Texture
Elallaqi

ABSTRACT

Enhancement of aeromagnetic data for qualitative purposes depends on the variations of texture and amplitude to outline various geologic features within the data. The texture of aeromagnetic data consists continuity of adjacent anomalies, size, and pattern. Variations in geology, or particularly rock magnetization, in a study area cause fluctuations in texture. In the present study, the anomalous features of Elallaqi area were extracted from aeromagnetic data. In order to delineate textures from the aeromagnetic data, the Red, Green, and Blue Co-occurrence Matrices (RGBCM) were applied to the reduced to the pole (RTP) grid of Elallaqi district in the South Eastern Desert of Egypt. The RGBCM are fashioned of sets of spatial analytical parameters that transform magnetic data into texture forms. Six texture features (parameters), i.e. Correlation, Contrast, Entropy, Homogeneity, Second Moment, and Variance, of RGB Co-occurrence Matrices (RGBCM) are used for analyzing the texture of the RTP grid in this study. These six RGBCM texture characteristics were mixed into a single image using principal component analysis. The calculated texture images present geologic characteristics and structures with much greater sidelong resolution than the original RTP grid. The estimated texture images enabled us to distinguish multiple geologic regions and structures within Elallaqi area including geologic terranes, lithologic boundaries, cracks, and faults. The faults of RGBCM maps were more represented than those of magnetic derivatives providing enhancement of the fine structures of Elallaqi area like the NE direction which scattered WNW metavolcanics and metasediments trending in the northwestern division of Elallaqi area.

1. Introduction

Aeromagnetic data are presently considered primary components of mineral investigation programs and are frequently being utilized for exploring petroleum. These datasets provide the mapping of varieties in rock magnetization. Wherever this magnetization is relatively strong and there are well-defined differences among units the process is notably powerful as a mapping mechanism (Dentith et al., 2000).

The definition of the texture is not easy however it is an inherent property of any image. Texture provides us by the information related to the spatial pattern of the tones or intensities in an image. It is a key attribute for many image analysis applications and it contains beneficial information concerning the deep structure of the area. So, the enhancement of texture can be employed to identify various spatial properties or patterns that are existing in the image. Geologic features like rock boundaries, dyke like structures, faults and fractures can be distinguished on processed filtered grids (such as Tilt derivative map) of the RTP data. However, these features are often difficult to be delineated on original magnetic maps but the can be much more reliably recognized on the magnetic texture maps. Textures obtained from magnetic maps indicate variations in physical properties and magnetic intensities of rocks including changes in geologic structures and rock composition (Hassan and Goussev, 2011).

* Corresponding author.
E-mail address: ahmed.dswky@sci.svu.edu.eg (A.M. Eldosouky).
Peer review under responsibility of National Research Institute of Astronomy and Geophysics.

Production and hosting by Elsevier

https://doi.org/10.1016/j.nrjag.2017.12.006
2090-9977/

Textures performed on aeromagnetic texture data reveal variations in physical characteristics of rock units including differences in geologic structures and types of rocks. Haralick et al. (1973) introduced a set of powerful analytical features to estimate multiple properties of an image character. These statistical features are regularly assigned to them as Co-occurrence Matrices (CM) and utilized widely by experts since 1973 for analyzing the texture, segmentation, and classification of the image. We applied CM to the magnetic RTP data of the in Red, Green, and Blue (RGB) form to create RGBCM texture images of Elallaqi region.

Elallaqi territory has been studied by many researchers like Eldosouky et al. (2017) who studied the area using aeromagnetic and remote sensing data to produce a mineral potential image of Elallaqi area. El Shimi (2005) and Abdel Salam and Stern (1996) investigated the structural pattern and zones of alteration of Elallaqi area. Elkhateeb and Eldosouky (2016) used aeromagnetic data to study the relation of porphyry intrusions to mineralization at Elallaqi region.

Texture analysis of aeromagnetic data in Elallaqi area, that can be used for geologic mapping and for identifying fine structures, is the main aim of the present study.

2. Geologic setting

Elallaqi district (Fig. 1a) extends between latitudes 22°22′50″ and 23°00′00″N, and longitudes 33°15′ and 34°15′ E covering an area about 7050 km2 in the South Eastern Desert of Egypt. Elallaqi territory is dominated by the Allaqi-Heiani suture (Stern et al., 1989; Stern, 1994; Abdelsalam and Stern, 1996). The main structural trends dominating Elallaqi district are the NW, NE, and NNE directions (Ramadan and Sultan, 2004) and Elallaqi area is dominated by the shear zone that was progressed amongst the four Neoproterozoic deformation grades (Abdelsalam and Stern, 1996). Elkhateeb and Eldosouky (2016) and Eldosouky et al. (2017) studied the shallow and deep geologic structures in Elallaqi area. These structures describe the favorable positions of hydrothermal movements; therefore, Enhancements of the satellite images were utilized to Elallaqi district to classify the regions of alteration.

Elallaqi area (Fig. 1b) occupied by the Mesozoic volcanic and sub-volcanic, Cretaceous sandstone, and basement crystalline rocks (Geologic map of Wadi Gabjabah Quadrangle, Egypt, 1996).

The southwestern part of Elallaqi area is occupied by the Cretaceous sequences including Abu Sumbul, Al Jilf, Abu Ajjaj, and Al Burj Formations whilst the wadies are filled by Quaternary sediments. The basement rocks occupy the majority of Elallaqi district. Island-arc, Late to post-tectonic granitoids, and Ophiolitic assemblages are the main basement types that occupy Elallaqi area.

The central part of Elallaqi territory is occupied by the ophiolitic assemblages which are composed of metagabbros, talc carbonate schist, and serpentinites. The island-arc assemblages are formed of meta-sedimentary and metavolcanic layers that are intruded by plugs of gabbro and diorite. Diorite, gabbro, quartz-diorite, and tonalite are the main constituents of the gabbro-diorite plugs. Island-arc assemblages are less numerous than meta-sedimentary and metavolcanic rocks. El-Nisr (1997) studied the geochemical characteristics of the metavolcanics which showed that there are transitional circumstances between continental-arc and continental margin. The late-post tectonic granitoids have an abundant presence in the central part of Elallaqi area, especially at Wadi El Shelman (Fig. 1b). They appear as separated circular eroded cliffs that are displayed by recent sand deposits.

3. Materials and enhancement techniques

3.1. Aeromagnetic data

Fig. 2 shows The magnetic intensity (TMI) or magnetic anomaly map of Elallaqi area used in the present investigation was acquired from the Egyptian Mineral Resources Authority that was accomplished by Aero Service Company (1984). The Aeromagnetic surveying was operated with a 120 m flight elevation and an average magnetic inclination of 32.8 N and declination of 1.9 E. So as to apply the RGBCM technique, a pole reduction (RTP) enhancement was applied to magnetic anomaly (TMI) map (Fig. 3).

RTP enhancement is applied to TMI data of Elallaqi territory to reduce or even decrease the distortion of the magnetic anomalies and makes the magnetic sources appear as if located at the pole and to change the asymmetric pattern of the anomalies to the symmetric mode (Baranov, 1957).

3.2. Co-occurrence Matrix Filtering (CM)

A set of flexible and important mathematical features, that were adopted to calculate different texture characteristics of an image, was explained by Haralick et al. (1973). The textural properties of the aeromagnetic grids were qualified in the present work using a technique based on co-occurrence matrices (CM). Dentith and

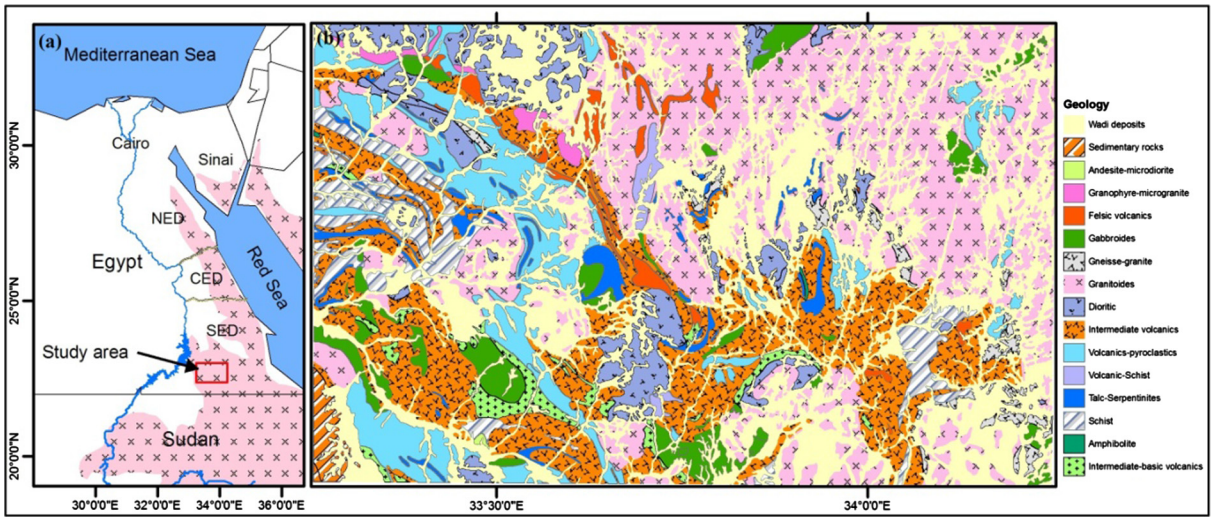

Fig. 1. (a) Regional geology of the Eastern Desert of Egypt, (b) Geologic map of Elallaqi territory (After EGSMA., 1996).

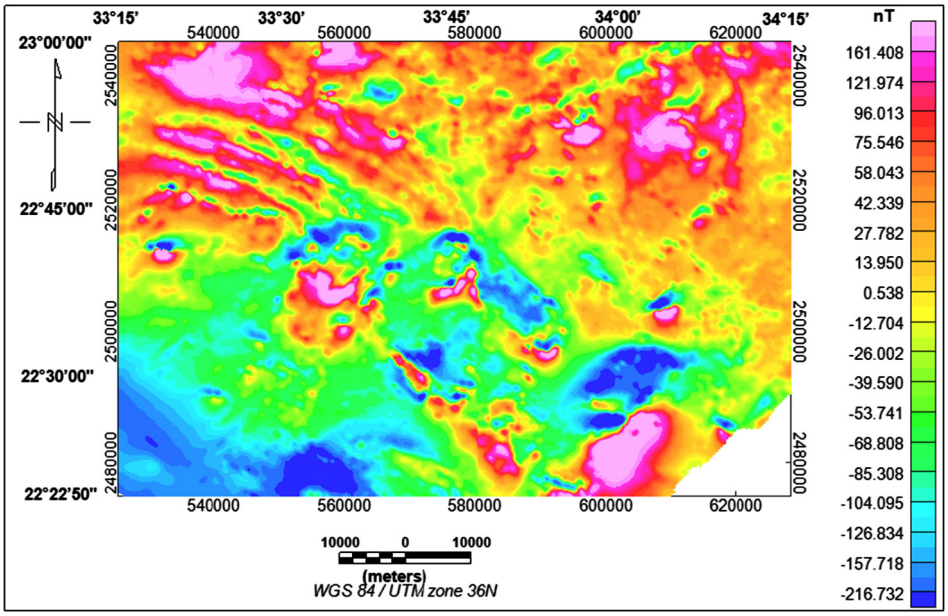

Fig. 2. Magnetic anomaly map of Elallaqi area.

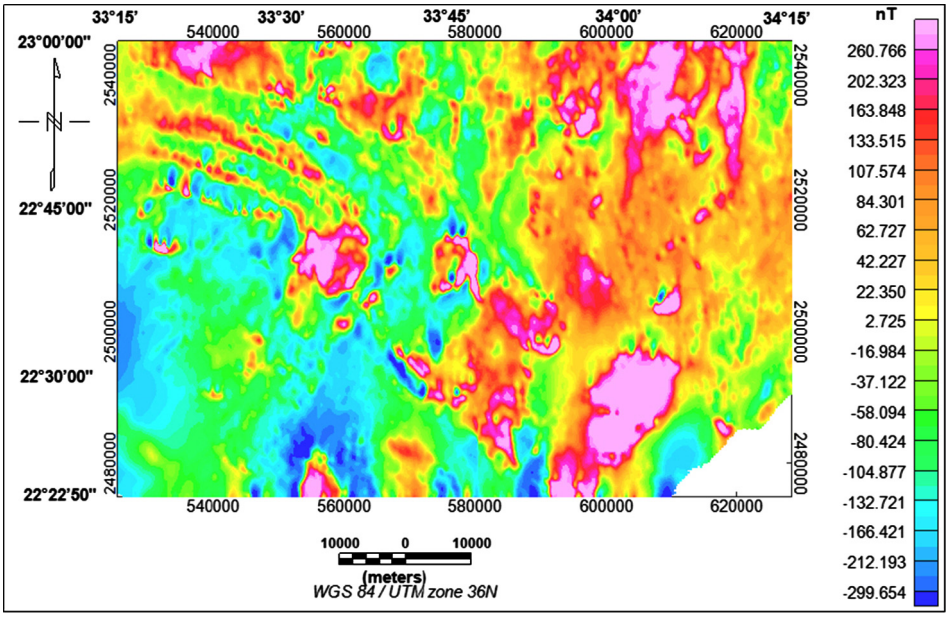

Fig. 3. RTP magnetic map of Elallaqi area.

Cowan (1997) and Dentith (1995) illustrated the principles and utilization of CM-based technique of aeromagnetic images. Firstly, the computation of CMs was defined by Haralick et al. (1973), who introduced them as a process for qualifying textures as wished for classifying image automatically. These analytical features are utilized widely by researchers for analyzing the texture, apportionment, and analysis of an image.

In the CM, a series of the probable color or intensity values were described as columns and rows in a 2D array. Statistically, The CM is a simple 2D histogram, which is a popularization of the 1D histogram (Dentith, 1995).

The characteristics of an image relevant to second-order statistics and probability which estimate the connection between pixels are measured using the co-occurrence texture enhancement (Srinivasan and Shobha, 2008).

The construction of co-occurrence requires two parameters. These two parameters are the orientation and displacement vector. For example, we want to introduce the two parameters of the CM of given image that have a window size of n x n. Where the orientation is 0 degree and displacement vector is 1 horizontal pixel. The CM size in this example is 3×3 (Table 1).

Relying on the two parameters, the CM will be populated. This population describes the occurrence of the similar sets of intensity within the CM. Table 2 displays the CM of the image shown in Table 1. At the location (0,0), number 5 indicates that we have 5 pairs of (0,0) at 1-pixel displacement in the horizontal direction. Moreover, at the location (2,2), the number 2 illustrates that we have 2 pairs of (2,2) at 1-pixel displacement in the horizontal direction. So, we can delineate the discontinuities in magnetic intensity using the CM.

Table 1
Given image.

1	1	0	0
0	0	0	0
1	1	2	2
0	0	2	2

Table 2
CM of the image in Table 1.

	0	1	2
0	5	1	1
1	1	2	1
2	1	1	2

14 analytical features for delineating the texture using co-occurrence matrices (CM) from images were proposed by Haralick et al. (1973). Out of this 14 texture features, only six are chosen and represented in the Red, Green, and Blue style (RGBCM) for this study. The applied CM features to Elallaqi data are the Correlation, Homogeneity, Second Moment, Entropy, Contrast, and Variance.

3.2.1. Correlation

The linear dependency and joint probability of the adjacent pairs of pixels are estimated by Correlation. Digital data Correlation is an optical technique that operates tracking & image registration techniques for accurate measuring of 2D and 3D variations in images. It can be also utilized for the displacement, deformation, and strain measurements (Mohanaiah et al., 2013).

$$Correlation = \sum_{i=0}^{N-1}\sum_{i=0}^{N-1}\frac{(i-\mu_i)(j-\mu_j)}{\sqrt{(\sigma_i^2)(\sigma_j^2)}}p_{i,j} \quad (1)$$

where $p_{i,j}$ is the insertion in a normalized tone spatial reliance pattern, N is the number of distinguished tone level in the enhanced image, μ_i, μ_j, σ_i and σ_j are the standard and means deviations of p_i and p_j.

3.2.2. Variance

Variance is a measurement of the dispersion of the digital number (DN) with regard to the mean value within a moving window (Woodcock and Harward, 1992).

$$Variance = \sum_i\sum_j (i-\mu)^2 p_{i,j} \quad (2)$$

3.3. Contrast

Contrast determines the amount of local variations existing in the image. The Contrast is zero when the adjacent pixels have the constant value. Therefore, The differences in intensities will increase the Contrast of magnetic data (Hassan and Goussev, 2011).

$$Contrast = \sum_{i=0}^{N-1}\sum_{j=0}^{N-1}(i-j)^2 p_{i,j} \quad (3)$$

3.4. Entropy

Entropy calculates the amount of complexity and shows the information of an image. The high value of image Entropy indicates that it has a great contrast between the adjacent pixels. High Entropy reflects the complex textures of the image (Mohanaiah et al., 2013).

$$Entropy = \sum_{i=0}^{N-1}\sum_{j=0}^{N-1} p_{i,j}(logp_{i,j}) \quad (4)$$

3.5. Homogeneity

Homogeneity correlates to the contrast of the texture. Homogeneity of an image will be at its highest value when the elements of the image are the same (Hassan and Goussev, 2011).

$$Homogeneity = \sum_{i=0}^{N-1}\sum_{j=0}^{N-1}\frac{p_{i,j}}{1+(i-j)^2} \quad (5)$$

3.6. Second Moment

The homogeneity of an image is measured by Uniformity or Second Moment. Second Moment will be at its highest value in images that have similar pixels. Second Moment is high in the homogeneous image which has great similarities among its adjacent pixels (Hassan and Goussev, 2011).

$$Second\ moment = \sum_{i=0}^{N-1}\sum_{j=0}^{N-1} p_{i,j}^2 \quad (6)$$

3.7. Principle component analysis (PCA)

Principal component analysis (PCA) is a powerful enhancement which used to transform the multidimensional data into simple information of a dataset. PCA was utilized to decrease the repetition of information that exists between the different grids (Loughlin, 1991; Gomez et al., 2005). Crosta and Moore (1989) explained the Feature-Oriented Principal Components Selection (FPCS), which depends on the study of PCA eigenvector reading to choose which of the principle component images allowed combining data directly concerning with the general spectral signatures of specific objectives. The images of the relevant principal component could show the objective regions in light or dark pixels (Loughlin, 1991). The PCA uses eigenvectors of the covariance pattern to produce a unitary convert pattern. This pattern is utilized to each pixel vector and converts it into a new vector with uncorrelated components ordered by variance (Stefanou, 1997).

4. Results and discussions

The texture is extremely complicated to describe although it is an essential characteristic of any image (Dentith, 1995). The information about spatial properties of the intensities or tones of an image can be illustrated from the texture. It is a key attribute for various image interpretation applications and it contains advantageous information related to the deep structure of an area. So, the texture study can be utilized to analyze various spatial properties or patterns that are existing in the image. Geologic features like rock boundaries, dike-like structures, faults, and fractures can be distinguished on processed filtered grids (such as Tilt derivative map) of the RTP grid. However, these features are often difficult to be delineated on original magnetic maps but they can be much more reliably recognized on the magnetic texture maps. Textures obtained from magnetic maps indicate variations in physical properties and magnetic intensities of different rock types including changes in geologic structures and rock types (Hassan and Goussev, 2011).

The textural properties of the aeromagnetic data of Elallaqi area were interpreted qualitatively using Co-occurrence Matrices method (CM). For the aeromagnetic data, computing CM texture measures at one location (x, y) yield localized features at that

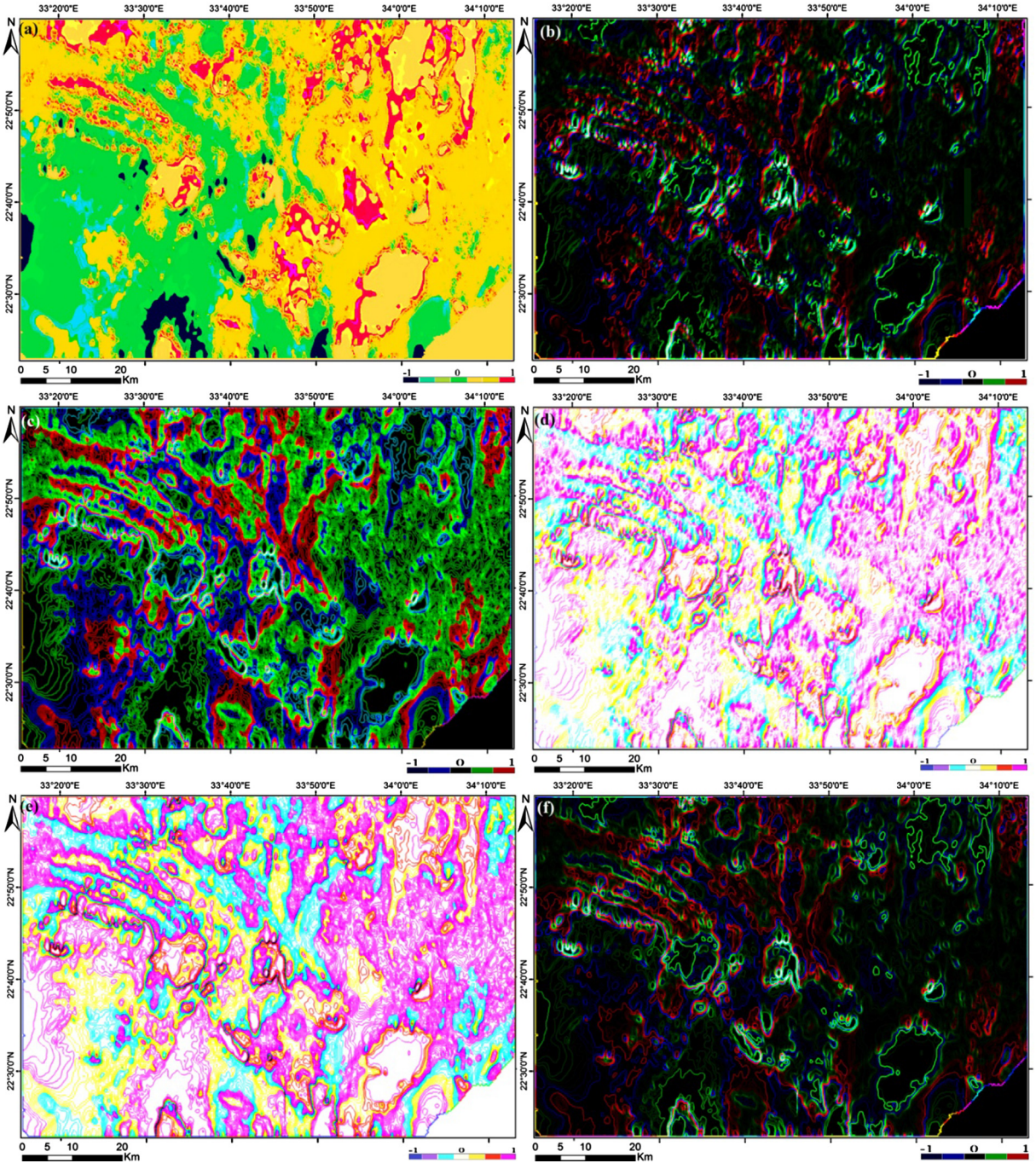

Fig. 4. RGBCM of RTP grid: (a) Correlation; (b) contrast; (c) entropy; (d) homogeneity; (e) Second Moment; (f) variance.

Table 3
PCA of the six RGBCM of the RTP grid.

Variance	Second Moment	Homogeneity	Entropy	Contrast	Correlation	Eigen-vector
0.393517	−0.78628	0.332976	−0.11916	0.222928	−0.09587	PC1
0.01798	−0.02368	0.00852	−0.23184	0.449056	−0.188872	PC2
−0.14321	0.277193	−0.13388	−0.35114	0.653288	−0.292489	PC3
−0.23128	−0.35136	−0.53402	−0.23416	−0.29034	−0.339519	PC4
0.321001	−0.16191	−0.7613	0.124706	0.199135	0.319748	PC5
0.075291	0.04378	0.021858	−0.01308	0.2329	0.568361	PC6

point. According to Kapur et al. (1985), by repeating the calculation of these measures in a regular manner or in scanning windows throughout the data set, the data are converted into matrices of the textural feature.

Six RGBCM texture features, i.e. Correlation, Contrast, Entropy, Homogeneity, Second Moment, and Variance, of RGB Co-occurrence Matrices (RGBCM) are used for analyzing the texture of the RTP grid at Elallaqi area. These RGBCM features are

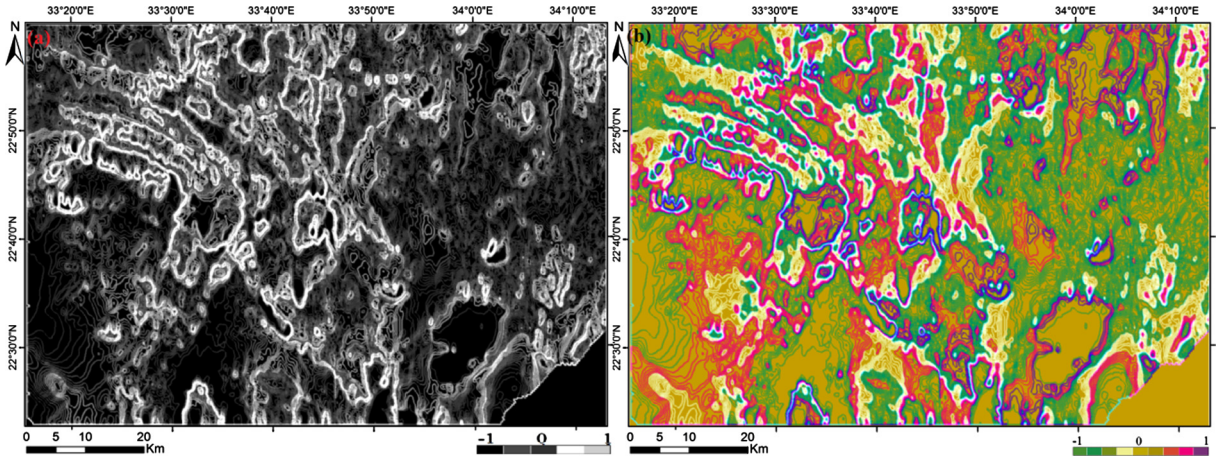

Fig. 5. (a) PC3 of RGBCM of RTP grid; (b) PC1, PC2 and PC3 (in RGB) of RGBCM of RTP grid.

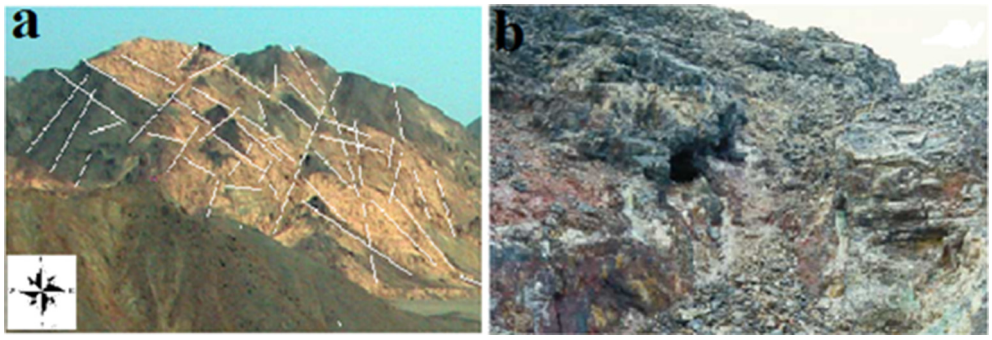

Fig. 6. Field photographs of (a) Field lineaments (b) Alteration zone.

measured in the same way as filtering by computing texture values on a moving window with a distinct size (3 × 3 window size) and selecting a rate to each of the image pixels identical to window centers.

Fig. 4 shows the application of six RGBCM of the RTP grid in Elallaqi territory. Zero values in the color bars of Fig. 4 indicate low-contrast parts in the images with no great variation in the matrix. The crucial investigation of these features shows that they have great similarities with minor variations among themselves. In Fig. 4, it can be noticed that the Entropy, the Second Moment, and the Variance images (Fig. 4c, e, and f) get high to abrupt changes. It is seen that the RGBCM-based Entropy, Variance, and Second Moment are more efficient to the aeromagnetic data in enhancing abrupt changes like edges, lineaments, sharp gradient belts and distorted anomalies. Moreover, it is observed that the Entropy, Variance, and Second Moment are more effective than the Correlation, Contrast, and Homogeneity (Fig. 4a, b, and d) in interpreting distortion and lineaments and that the area-based 'equality' or homogeneity are highlighted in the Entropy image. The differences of the anomalies indicate that the RGBCM and its statistics are promising in differentiating the magnetic anomalies.

In order to combine all the six maps into a single map illustrating all the interesting features of the study area, principal component analysis (PCA) was applied to the RGBCM images. Examining the eigenvector values of the PCA loading of the selected six features demonstrate that PC3 shows the largest total variations (Table 3) as shown in Fig. 5(a). The first three principal components are represented in RGB map (Fig. 5b) to be used for mapping texture variations (Zero values in the color bar indicate low-contrast).

Figs. 4 and 5 show several interesting geologic features in a way more clearer than the maps obtained through the utilization of derivative filters. The results reveal several geologic features such as lithologic contacts and boundaries between different rock units in Elallaqi area like the boundaries between metasediments and metavolcanics which cover the northwestern region of Elallaqi territory and also contacts between granitoids and its surroundings in the eastern portion of Elallaqi area. The faults and fractures of RGBCM maps are more obvious and represented than those of magnetic derivatives providing enhancement of the fine structures of Elallaqi area like the NE direction which scattered WNW metavolcanics and metasediments trending in the northwestern division of Elallaqi area. Also, porphyry intrusions and dike-like structures can be easily distinguished from texture analysis such as those that trending NE in the eastern and southern parts of Elallaqi territory.

The resulted texture obtained from RGBCM maps was correlated with the real geologic features around metavolcanics and metasediments at the northwestern part of Elallaqi area (Fig. 6). Based on field observation at Wadi Hadaiyib (Lat. 22°50′20.19″N, Long. 33°19′46.65″E), the predominant WNW and NW directions scattered by NE (Fig. 6a) clearly appear and being strongly matched with RGBCM results. Moreover, Fig. 6b shows an alteration zone with multi-colored units related to altered metavolcanics that lie between latitude 22°51′23.69″N and longitude 33°23′37.11″E which was presented as a zone of high texture variations in the RGBCM maps.

5. Conclusions

The textural features based on CM can be a beneficial tool in the enhancement and interpretation aeromagnetic data. The application

of RGBCM to the aeromagnetic data of Elallqi territory helps to delineate the boundaries, circular and linear features that extend in any direction.

The shallow texture maps of Elallaqi territory appear to be very effective in the visualization of various geologic features. The good inspection of the results manifests well-defined geologic characteristics and helps for geologic mapping and delineating fine scale structures than those of original aeromagnetic grids.

References

Abdelsalam, M.G., Stern, R.J., 1996. Sutures and shear zones in the Arabian-Nubian Sheild. J. Afr. Earth Sc. 23, 289–310.

Aero Service Report, 1984. Training course in airborne magnetic and radio-metric surveying. Presented to the Egyptian General Petroleum Corporation, Cairo, Egypt.

Baranov, V., 1957. A new method for interpretation of aeromagnetic maps: pseudo-gravimetric anomalies. Geophysics 22, 359–383.

Crosta, A.P., Moore, J. McM., 1989. Enhancement of Landsat Thematic Mapper Imagery for Residual Soil Mapping in SW MinaisGerais State, Brazil: A Prospecting Case History in Greenstone Belt Terrain. In: Proceedings of the 7th(ERIM) Thematic Conference: Remote Sensing for Exploration Geology, Calgary, 2–6 Oct., pp 1173–1187.

Dentith, M.C., 1995. Textural filtering of aeromagnetic data. Expl. Geophys. 26, 209–214.

Dentith, M.C., Cowan, D.R., 1997. Enhancement of aeromagnetic data using grey level co-occurrence matrices. ASEG Preview 69, 12–14.

Dentith, M.C., Cowan, D.R., Tompkins, L.A., 2000. Enhancement of subtle features in aeromagnetic data. Explor. Geophys. 31 (1/2), 104–108.

Eldosouky, A.M., Abdelkareem, M., Elkhateeb, S.O., 2017. Integration of remote sensing and aeromagnetic data for mapping structural features and hydrothermal alteration zones in Wadi Allaqi area, South Eastern Desert of Egypt. J. Afr. Earth Sc. 130, 28–37.

Elkhateeb, S.O., Eldosouky, A.M., 2016. Detection of porphyry intrusions using analytic signal (AS), Euler Deconvolution, and Center for Exploration Targeting (CET) Technique Porphyry Analysis at Wadi Allaqi Area, South Eastern Desert, Egypt. Int. J. Sci. Eng. Res. 7 (6), 471–477. ISSN 2229-5518.

El-Nisr, S.A., 1997. Late Precambrian volcanism at Wadi Allaqi, SE Desert, Egypt: evidence for continental arc/continetal margin environment. J. Afr. Earth Sc. 24, 301–313.

El-Shimi, K.A., 2005. Application of remote sensing in mineral exploration at Wadi Allaqi district, SW-Eastern Desert of Egypt. Ann. Geol. Surv. Egypt. XXVIII, 205–223.

Geologic map of Wadi Jabjabah Quadrangle, Egypt, 1996, Scale 1: 250 000, EGSMA.

Gomes, C., Delacourt, C., Allemand, P., Ledru, P., Wackerle, R., 2005. Using Aster remote sensing data set for geological mapping, in Namibia. Phys. Chem. Earth, Parts A/B/C 30 (1–3), 97–108.

Haralick, R.M., Shanmugam, K., Dinstein, I., 1973. Textural features for image classification. IEEE Trans. Syst. Man. Cybern. SMC-3, 610–621.

Hassan, H.H., Goussev, S., 2011. Texture analysis of high resolution aeromagnetic data to identify geological features in the horn River Basin, NE British Columbia. In: Conference Paper, Recovery –CSPG CSEG CWLS Convention.

Kapur, J.N., Sahoo, P.K., Wong, A.K.C., 1985. A new method for graylevel picture thresholding using the entropy of the histogram. Comput. Vision Graph. Image Process. 29, 273–285.

Loughlin, W.P., 1991. Principal component analysis for alteration mapping. Photogramm. Eng. Rem. Sens. 57, 1163–1169 (Thematic Conference on Remote Sensing, Denver, USA).

Mohanaiah, P., Sathyanarayana, P., GuruKumar, L., 2013. Image Texture Feature Extraction Using GLCM Approach. Int. J. Sci. Res. Publ. 3 (5). ISSN 2250-3153.

Ramadan, T.M., Sultan, S.A., 2004. Integration of remote sensing, geological and geophysical data for the identification of massive sulphide zones at Wadi Allaqi area, South Eastern Desert, Egypt. M.E.R.C. Ain Shams Univ. Earth Sci. Ser. 18, 165–174.

Srinivasan, G.N., Shobha, G., 2008. Statistical texture analysis. In: Proceedings of World Academy of Science, Engineering and Technology, vol. 36, ISSN 2070-3740.

Stern, R.J., Kroner, A., Manton, W.I., Reischmann, T., Mansour, M., Hussein, I.M., 1989. Geochronology of Late Precambrian Hamisana shear zone, Red Sea Hills, Sudan and Egypt. J. Geol. Soc. Lond. 146, 1017–1030.

Stern, R.J., 1994. Arc assembly and continental collision in the Neoproterozoic East African Orogen: implications for consolidation of Gondwanaland. Ann. Rev. Earth Planet. Sci. 22, 319–351.

Stefanou, M.S., Olsen, R.C., Cristi, R., 1997. A Signal Processing Perspective of Hyperspectral Imagery Analysis Techniques, Master's Thesis, Naval Postgraduate School, Monterey, California.

Woodcock, C.E., Harward, V.J., 1992. Nested-hierarchical scene models and image segmentation. Int. J. Rem. Sens. 13, 3167–3187.